UC Santa Cruz
UC Santa Cruz Electronic Theses and Dissertations

Title

Synthesis And Structure-Activity Relationships Studies Of 4-((4-Hydroxy-3-Methoxybenzyl)Amino)Benzenesulfonamide Derivaties As Potent And Selective Inhibitors Of 12-Lipoxygenase

Permalink

Author

Sowell-Kantz, Auric

Publication Date

2014

Peer reviewed|Thesis/dissertation

UNIVERSITY OF CALIFORNIA

SANTA CRUZ

SYNTHESIS AND STRUCTURE-ACTIVITY RELATIONSHIPS STUDIES OF 4-((4-HYDROXY-3-METHOXYBENZYL)AMINO)BENZENESULFONAMIDE DERIVATIES AS POTENT AND SELECTIVE INHIBITORS OF 12-LIPOXYGENASE

A thesis submitted in partial satisfaction
of the requirements for the degree of

MASTER OF SCIENCE

In

CHEMISTRY

By

Auric Sowell-Kantz

March 2014

The Thesis of Auric Sowell-Kantz

Is approved:

_____
Professor William Scott, Chair

_____
Professor Theodore Holman

_____
Professor Seth Rubin

_____
Tyrus Miller
Vice provost and Dean of Graduate Studies

TABLE OF CONTENTS:

LIST OF FIGURES

Abstract

SYNTHESIS AND STRUCTURE-ACTIVITY RELATIONSHIPS STUDIES OF 4-((4-HYDROXY-3-METHOXYBENZYL)AMINO)BENZENESULFONAMIDE DERIVATIES AS POTENT AND SELECTIVE

Auric Sowell-Kantz

Human lipoxygenases (LOXs) are a family of iron-containing enzymes which catalyze the oxidation of polyunsaturated fatty acids to provide the corresponding bioactive hydroxyeicosatetraenoic acid (HETE) metabolites. These eicosanoid signaling molecules are involved in a number of physiologic responses such as platelet aggregation, inflammation, and cell proliferation. Our group has taken a particular interest in platelet-type 12-(*S*)-LOX (12-LOX) because of its demonstrated role in skin diseases, diabetes, platelet hemostasis, thrombosis, and cancer. We previously reported the discovery of **ML127**, a potent and selective 12-LOX inhibitor which has proven to be a valuable tool compound for researchers in the field. However, the limited tolerance for structural modification and modest PK profile for this chemotype prompted us to continue our discovery efforts toward novel 12-LOX inhibitors. Herein, we report the identification and medicinal chemistry optimization of a 4-((2-hydroxy-3-methoxybenzyl)amino)benzenesulfonamide-based scaffold. Top compounds, exemplified by **35** (**ML355**) and **36,** display nM potency against 12-LOX and excellent selectivity over related lipoxygenases and cyclooxygenases. In addition to possessing favorable ADME properties, **35** and **36** inhibit PAR-4 induced aggregation and calcium mobilization in human platelets, and reduce 12-HETE in mouse/human beta cells.

INTRODUCTION:

Lipoxygenases are a class of non-heme iron-containing enzymes which regio- and stereospecifically oxidize polyunsaturated fatty acid substrates such as arachidonic acid (AA) and linoleic acid (LA).[i] The position at which these *cis*, *cis*-1,4-pentadiene substrates are oxidized correspond to the requisite lipoxygenase, with the three major human lipoxygenases: 5-LOX, 12-LOX, and 15-LOX-1, oxidizing the C-5, C-12 and C-15 positions respectively. Lipoxygenases are involved in the first committed step in a cascade of metabolic pathways and the products of these enzymes (eicosanoids) are precursors of hormones such as leukotrienes and lipoxins, which mediate a wide array of cellular functions.[ii] Consequently, the lipoxygenase enzymes and their bioactive metabolites (e.g. hydroxyeicosatetraenoic acid (HETE) and leukotriene A_4) have been implicated in a variety of inflammatory diseases and cancers. Specifically, 5-LOX has been implicated in cancer[iii] and inflammatory diseases such as asthma[iv] and remains the only lipoxygenase enzyme for which there is an FDA-approved inhibitor (Zilueton) on the market.[v] Reticulocyte 15-LOX-1 has received particular attention for its role in atherogenesis,[vi] neurodegenerative diseases,[vii] and neuronal damage associated from an acute ischemic stroke event.[viii] 12-LOX exists as three isozymes, platelet-type, leukocyte, and epidermal, however leukocyte 12-LOX is not found in humans yet is present in rat, mouse, pig and cow.[ix] Platelet-type 12-(*S*)-LOX (12-LOX), which the current study focuses on, has been found to be overexpressed in a variety of tumor tissues including prostate cancer, colorectal cancer, breast cancer and lung cancer.[x] Moreover, 12-HETE levels have been linked

to increased cancer cell metastasis by facilitating tumor cell motility and angiogenesis.[xi] 12-LOX is also expressed in human pancreatic islets, which is upregulated and activated by inflammatory cytokines leading to increased 12-LOX translocation.[xii] The resulting 12-HETE product leads to reduced insulin secretion, reduced metabolic activity and pancreatic β cell death through the amplification of the inflammatory response.[xiii] Toward this end, both non-obese diabetic (NOD) 12-LOX[xiia] and 12-LOX KO[xiib] mice showed significant resistance to the development of diabetes compared to the controls, suggesting 12-LOX is a clear regulator in this disease. 12-LOX and its product 12-HETE have also been implicated in the modulation of hemostasis and thrombosis via their role in regulating platelet function (reactivity, clot formation, calcium mobilization).[xiv] Historically the precise role of 12-HETE has been controversial with reports suggesting both an anti- and pro-thrombotic effects.[xv] One difficulty in being able to clearly define the role of 12-LOX in these systems has been the lack of potent and selective 12-LOX small molecule inhibitors. However, working with the inhibitor, NCTT-956, which is similar to our previous series (**ML127**), we were able to show that inhibition of 12-LOX leads to reduced platelet aggregation and calcium mobilization following stimulation by various agonists (PAR1-AP, PAR4-AP, Collagen, thrombin).[xvi] These results helped further validate 12-LOX as a potential target for anti-platelet therapy.

Our laboratories[xvii] and others[xviii] have been actively engaged for many years in the discovery of novel potent 12-LOX inhibitors utilizing traditional medicinal chemistry, computational chemistry[xix] and natural product isolation.[xx] However, despite these

extensive efforts, no drug-like small molecule that was either chemically tractable or selective had been discovered. Instead, these efforts yielded compounds that were either reductive and/or promiscuous in nature, as exemplified by the inhibitors listed in Figure 1. The known reductive LOX inhibitor, nordihydroguaiaretic acid (NDGA)[xviia] and other natural products including the brominated aryl phenols[xviic] which are marine derived natural products, all have modest 12-LOX inhibitory activity (micromolar). Importantly, these compounds lack selectivity towards 12-LOX and have undesirable chemical structures. For example, the polyphenolic compound, Baicalein, was once one of the most commonly used 12-LOX inhibitors as it was originally thought to be selective for 12-LOX. However, subsequent studies revealed equipotent *in vitro* activity towards both 12-LOX and 15-LOX-1.[xviib]

Given the previously stated biological importance of 12-LOX and the lack of high quality probe compounds in the literature, we initiated a high throughput screening campaign as part of the MLPCN program. This effort led to the discovery of an 8-Hydroxyquinoline based compound (**ML127**) which exhibited excellent selectivity, >50-100 fold selectivity over related lipoxygenses and cyclooxygenase. In contrast to many of the previously reported inhibitors, kinetic experiments revealed that these inhibitors were non-competitive and non-reductive. Chiral HPLC separation of the probe molecule revealed a chiral preference for activity with the (–)-enantiomer being much more potent than the (+)-enantiomer (<0.5 μM vs. >25 μM, respectively).[xxi] However, despite this promising activity the chemical series was difficult to optimize further, given that subtle structural modifications led to diminished activity.

Therefore, we sought to reexamine the results from the original HTS to uncover

additional compounds that may be amendable to medicinal chemistry optimization.

Ultimately, this led to the identification of a 4-((2-hydroxy-3-

methoxybenzyl)amino)benzenesulfonamide-based scaffold which was subjected to

medicinal chemistry optimization and biological characterization. The results of these
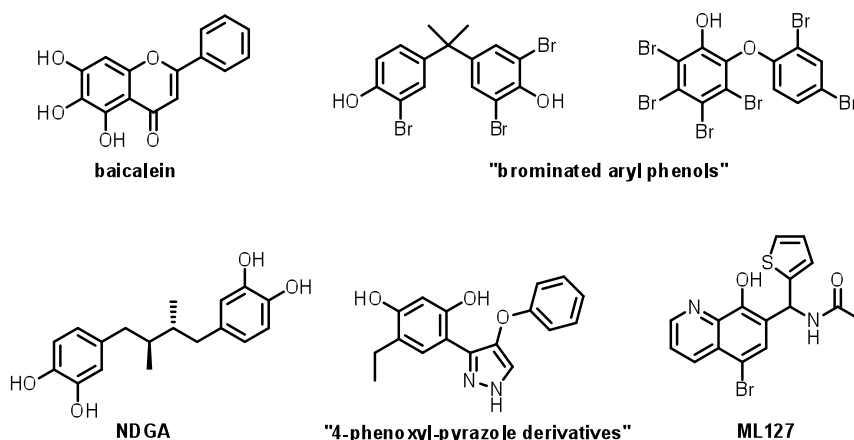
efforts are described herein.

Figure 1. Representative examples of previously reported 12-LOX inhibitors

CHEMISTRY:

Prior to initiating an extensive SAR campaign around the HTS "hit" molecule, (**1**),

the NIH first sought to resynthesize the molecule to confirm its identity and activity.

The synthesis of compound **1** involved a reductive amination with 4-

aminobenzesulfonmide and 2-hydroxy-3-methoxybezaldehyde. While this route

appeared amendable to the facile preparation of numerous synthetic analogs, the

standard mild method for reductive aminations utilizing sodium

triacetoxyborohydride and catalytic acetic acid afforded little to no product. Instead, a step-wise approach involving pre-formation of the imine was required with 4-amino-*N*-(thiazol-2-yl)benzenesulfonamide (**2**) and the requisite benzaldehyde overnight in ethanol at reflux. Subsequent reduction of the imine with sodium borohydride provided the desired compounds **1, 8-10** and **14-33** (Scheme 1, Method A). While this route worked for a majority of the analogs, some analogs (**11-13 & 34**) required an alternative route in which a Buchwald-Hartwig type coupling was utilized with the commercially available 4-bromo-*N*-(thiazol-2-yl)benzenesulfonamide (**3**) and 2-methoxy substituted benzyl amines to provide the desired products in a yields of 25-40% (Scheme 1, Method B).[xxii] For modifications of the thiazole portion of the molecule we wanted to introduce diversity in the final step of the synthesis (Scheme 1, Method C). Therefore, reaction of commercially available 4-aminobenzenesulfonamide (**4**) with 2-hydroxy-3-methoxybenzaldehyde in ethanol at reflux for 6 h, followed by treatment with sodium borohydride provided compound **5** in 95% yield. The resulting sulfonamide derivative was then subjected to Cu-catalyzed N-arylation conditions using the appropriate heteroaryl bromides to afford compounds **35, 38, 44-48, 52, 53, 56-59, 61-69, 71, 74,** and **75** in good yields.[xxiii] Despite the general versatility of this method, there was a few isolated cases where the Cu-catalyzed reaction failed to produce the desired product (e.g. compounds **77-83**), or the heteroaryl bromides were not readily available. For these compounds a less direct route was developed by heating 4-nitrobenzene-1-sulfonyl chloride (**6**) and the required heteroaryl amines to 100 $^{\circ}$C for 1.5 to 18 hours depending on the

reactivity of the amine to give the 4-nitrophenyl-sulfonamide derivatives **7** (Scheme 1, Method D). Reduction of the nitro group was achieved using the H-Cube® Pro flow reactor with 10% Pd on carbon at 50 °C and a pressure of 50 bar. Alternatively, for less soluble compounds which were not amenable to flow chemistry, a Zn/AcOH reduction was performed at 60 °C in methanol. Once the desired aniline was in hand a reductive amination was carried out with the corresponding benzyl amine derivative to provide compounds **36**, **37**, **39-43**, **49-51**, **54**, **55**, **60**, **70**, **72**, **73**, and **76-83**.
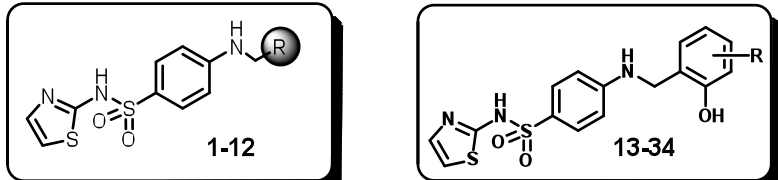
Scheme 1. Synthesis of analogs 1-83.
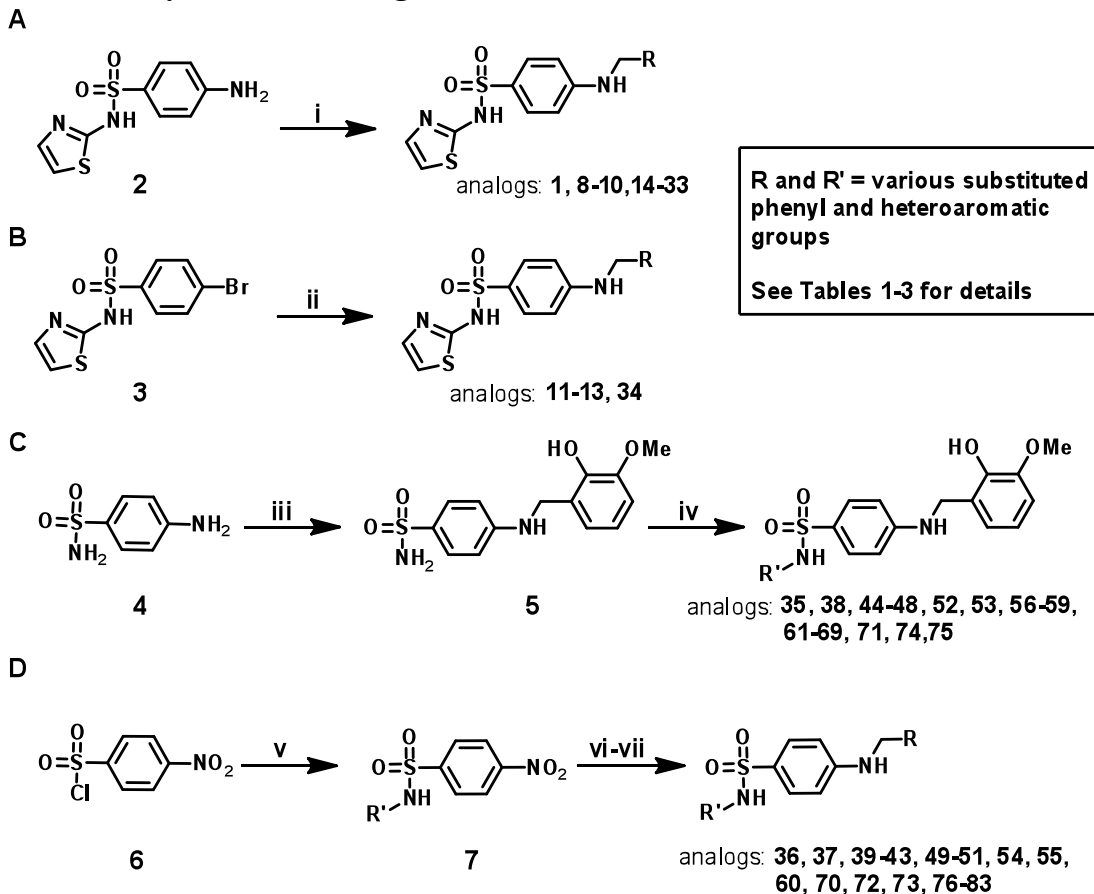
(i)   **R**CHO (1.5 equiv), EtOH, 3-18 h, reflux, NaBH$_4$ (3.0 equiv), 0.5-0.6 h at rt; (ii) **R**CH$_2$NH$_2$ (1.2 equiv), Xantphos (0.06 equiv), Pd$_2$dba$_3$ (0.02 equiv), NaO*t*Bu (2.5 equiv), 1,4-dioxane, MW, 30 min, 100 °C. (iii) 2-hydroxy-3-methoxybenzaldehyde (1.2 equiv), EtOH, 6 h, reflux, NaBH$_4$ (1.5 equiv),

30 min, rt, 95%. (iv) **R'**Br (1.2 equiv), N,N'-dimethylethylenediamine, CuI (0.05 equiv), K_2CO_3 (2.5 equiv), 80 $^{\circ}$C, 6-8 h. (v) **R'**NH_2, pyridine, 100 $^{\circ}$C, 1.5-18 h. (vi) 10% Pd/C, MeOH/EtOAc/THF (1:1:1), 50 bar, 50 $^{\circ}$C or zinc (4.0 equiv), AcOH (4.0 equiv), methanol, 60 $^{\circ}$C, 30 min-2 h. (vii) 2-hydroxy-**R**-benzaldehyde (1.2 equiv), EtOH, 18 h, reflux, $NaBH_4$ (3.0 equiv).

RESULTS AND DISCUSSION:

After having confirmed the identity and biological activity of the resynthesized lead compound **1**, the NIH and the Holman lab began our systematic SAR explorations as shown in Tables 1-3. Our initial concern surrounding this chemotype was the presence of the catechol-like moiety as this functionality can often be associated with promiscuous activity and/or metal chelation. However, the excellent selectivity of **1** over related lipoxygenase enzymes (5-LOX, 15-LOX-1 and 15-LOX-2) suggested this was not the case. Regardless, we chose to focus on modification of the 2-hydroxy-3-methoxybenzyl moiety for our first around of analog synthesis. As shown in Table 1, we found that removal of the phenolic groups (**8**), 3-OMe group (**9**), or the 2-OH group (**10**) resulted in a complete loss of activity. Protecting the 2-OH moiety as methyl ether (compounds **11-12**) or replacing with an amine (compounds **13** and **15**) also negated all 12-LOX inhibitory activity. We tried a bioisosteric replacement of the catechol moiety with an indole (**17**), however this analog was also inactive. These data seemed to indicate the requirement of the 2-OH group, yet this group alone was not enough for activity. Therefore, we decided to hold the 2-OH group constant and try modifications at the other positions. We found the 3-Cl (**19**, IC_{50} = 6.2 µM) to have comparable activity, while the 3-fluoro and 3-bromo (**20**, IC_{50} = 19

7

μM and **21**, $IC_{50} = 13$ μM) were ~4 to ~2.5-fold fold less active, respectively. An interesting and unexpected result was the 2-fold improvement in activity observed for the 4-bromo derivative (**22**, $IC_{50} = 2.2$ μM) and 4-chloro derivative (**27**), which had comparable activity (6.3 μM). In contrast, the 4-methoxy derivative (**28**) had reduced activity compared to compound **1** ($IC_{50} = 22$ μM). Other substituents at 3-position such as methyl (**23**), amino (**24**) and nitro (**25**) all resulted in a drastic loss of activity $IC_{50} > 40$ μM as did all 5-position analogs (**29-33**). Only one compound with a modification to the 6-position was synthesized, R = OMe (**34**) and this was also inactive. Thus, we determined the 2-OH to be essential for activity and the 3-position to be most optimal for the methoxy group. However, this preliminary SAR suggested that the 3-OMe could be replaced with a chloro group (**19**) and a 4-bromo (**22**) and 4-chloro (**27**) while maintaining comparable, if not improved activity to compound **1.**

Table 1. 12-LOX Inhibition of analogs 1, 8-34[a]

Compound	R	12-LOX IC$_{50}$ (μM)	Compound	R	12-LOX IC$_{50}$ (μM)
1	2-OH,3-OMe-Ph	5.1	19	3-Cl	6.2
8	Ph	>40	20	3-F	19
9	2-OH-Ph	>40	21	3-Br	13
10	3-OMe-Ph	>40	22	4-Br	2.2
11	2-OMe-Ph	>40	23	3-Me	>40
12	2,3-OMe-Ph	>40	24	3-NH$_2$	>40
13	2-NH$_2$-Ph	>40	25	3-NO$_2$	>40
14	3-OH-Ph	>40	26	3-vinyl	>40
15	2-NH$_2$,3-OMe-Ph	>40	27	4-Cl	6.3
16	3-OH,4-OMe-Ph	>40	28	4-OMe	22
17	7-indole	>40	29	5-Cl	>40
18	2,3-Cl-Ph	>40	30	5-OMe	>40
			31	5-NH$_2$	>40
			32	5-F	>40
			33	5-NO$_2$	>40
			34	6-OMe	>40

[a] IC50 values represent the half maximal (50%) inhibitory concentration as determined in the UV-Vis cuvette-based assay in triplicate. The error for these values are below 20%.

Having established a preliminary SAR profile of this region of the molecule, we next turned our attention to modification of the thiazole group as shown in Table 2. Gratifyingly, unlike our efforts on the phenyl moiety, changes to this region of the molecule led to analogs with improved potency. Replacing the thiazole moiety with a 2-benzothiazole (**35**, **ML355**) resulted in an 18-fold improvement in 12-LOX activity while retaining selectivity. The benzoxazole (**36**) and benzimidazole (**37**) possessed good to excellent activity, and introduction of a methyl group at the 4-position of the benzothiazole ring (**39**), maintained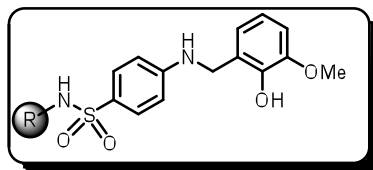 excellent 12-LOX activity (IC$_{50}$ = 0.24 μM). Potency against 12-LOX was also improved over 10-fold when the thiazole was

9

replaced with a thiophene (**38**), but the substituted thiazole/isoxazole derivatives (**40-43**) did not show this increased potency. The phenyl derivative (**48**), a known thiophene bioisostere, also demonstrated potent activity against 12-LOX (IC_{50} = 0.5 µM). Generally, larger aromatic [1-naphthalene (**49**) and 2-naphthalene (**50**)] and heteroaromatic compounds [3-quinoline (**46**), 8-isoquinoline (**47**), 2-pyridine (**58**) and 3-pyridine (**59**)] were well tolerated and had better potency than the thiazole derivative (**1**). In an effort to improve solubility by adding solubilizing functionality, we synthesized a few phenyl derivatives substituted with a piperazine moiety at different positions around the aryl ring (**53-55**). While these changes were tolerated, they had much reduced activity compared to the top actives (e.g. entry **35** and **36**).

Given our interest in pursuing multi-parameter optimization, we simultaneously tested many of these analogs for activity against 15-LOX-1 to ensure that selectivity was maintained. These compounds were initially tested against 15-LOX-1 at a single concentration (25 µM) and an IC_{50} was determined only on compounds of particular interest. These studies showed that replacement of the thiazole with a benzothiazole, and its derivatives maintained favorable selectivity with 15/12-LOX ratios of 29-fold (**35**), 18- (**39**), 19- (**62**) and 20- (**68**). The 15-LOX-1/12-LOX selectivity ratio improved to over 100 with conversion of the benzothiazole to a benzoxazole (**36**), benzimidazole (**37**) and *m-i*Pr substituted phenyl (**67**). Interestingly, the phenyl substitution (**48**) only had a selectivity ratio of 15. A wide-range of selectivity was observed despite the compounds bearing comparable structures, ranging from almost complete inhibition of 15-LOX-1 (e.g. **38** and **63**) to minimal inhibition (e.g. **55**, **58**,

and **66**). The dramatic effect on selectivity between 12-LOX and 15-LOX-1 in this portion of the molecule supports the differences between the active sites of the two LOX isozymes, as seen previously by mutational analysis.[xxiv]
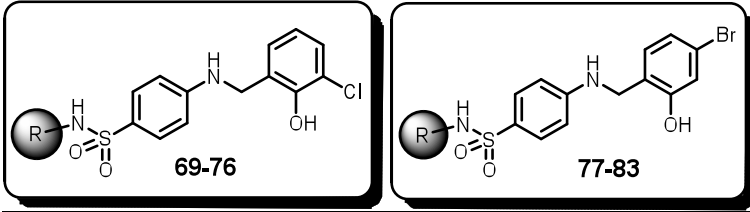
Table 2. 12-LOX Inhibition of analogs 35-68[a]

Compound	R	12-LOX IC$_{50}$ (μM)	15-LOX-1 IC$_{50}$ (μM)	% inh[b]
35 (ML355)	2-benzothiazole	0.34	9.7	—
36	2-benzoxazole	0.79	>100	—
37	2-benzimidazole	0.57	>100	—
38	2-thiophene	0.35	—	100
39	4-Me-2-benzothiazole	0.24	4.2	—
40	4-Me-2-thiazole	2.8	—	14
41	5-Me-2-thiazole	3	—	75
42	5-Ph-2-thiazole	91%[b]	—	77
43	4,5-Me-2-thiazole	1.4	—	37
44	5-Me-3-isoxazole	11	—	—
45	3-OMe-Ph	85%[b]	—	73
46	3-quinoline	0.48	—	77
47	8-isoquinoline	0.70	—	70
48	Ph	0.50	7.6	—
49	1-naphthalene	0.51	—	73
50	2-naphthalene	0.33	—	54
51	1,4-bi-Ph	1.3	—	60
52	1,3-bi-Ph	82%[b]	—	70
53	3-piperazine-Ph	3.5	—	31
54	4-piperazine-Ph	11	—	—
55	4-piperidine-Ph	3.7	—	8
56	4-piperazine-3-pyr	4	—	12
57	4-methyl-3-pyr	5	—	18
58	2-pyr	5	—	3
59	3-pyr	7	—	—
60	2-pyrimidine	12	—	—
61	3-[t]Bu-Ph	0.39	—	66
62	6-methoxy-2-benzothiazole	0.26	5.1	—
63	4-Ph-2-thiazole	0.18	—	87
64	3-morpholine-Ph	3.8	—	50
65	4N-boc-piperidine-3-Ph	0.76	—	34
66	3-piperidine-Ph	1.1	—	4.7
67	3-iPr-Ph	0.16	>100	—
68	6-F-2-benzothiazole	0.22	4.5	—

As noted above (Table 1), replacement of the "right-hand" portion of the molecule with a 3-chloro-2-phenol (**19**), 4-bromo-2-phenol (**22**) or 2-chloro-2-phenol (**27**), resulted in comparable potency to **1** with IC$_{50}$ values of 6.2, 2.2 and 6.3 µM respectively. Therefore, we sought to explore a matrix library utilizing these groups with some of the best sulfonamide derivatives discovered as part of the initial SAR efforts (see Table 3, compounds **69-83**). Unfortunately, none of the compounds had improved potency. Generally, the 2-benzothiazole moiety gave the best activity with both the 3-chloro-2-phenol (**71**; IC$_{50}$ = 1.3 µM) and 4-bromo-2-phenol (**79**; IC$_{50}$ = 1.7 µM), although the 1-naphthalene derivative **78** also had comparable potency (IC$_{50}$ = 1.3 µM).

Table 3. 12-LOX Inhibition of analogs 69-83[a]

| Compound | R | 12-LOX | 15-LOX-1 | |
		IC$_{50}$ (μM)	IC$_{50}$ (μM)	% inh[b]
69	Ph	4.5	—	49%
70	1-naphthalene	1.6	—	70%
71	2-benzothiazole	1.3	7.6	—
72	2-naphthalene	2.3	—	75%
73	4-bi-Ph	4.2	—	73%
74	8-isoquinoline	4.5	—	63%
75	3-quinoline	5.3	—	58%
76	4-Ph-piperidine	6.3	—	4%
77	Ph	2.9	—	82%
78	1-naphthalene	1.3	—	83%
79	2-benzothiazole	1.7	—	100%
80	3-quinoline	2.3	—	74%
81	2-naphthalene	2.2	—	78%
82	4-bi-Ph	2.5	—	80%
83	8-isoquinoline	5.6	—	55%

[a] IC$_{50}$ values represent the half maximal (50%) inhibitory concentration as determined in the UV-Vis cuvette-based assay in triplicate. The error for these values are below 20%. [b] represents percent inhibition at 25 μM.

The results of our SAR investigations, which provided compounds with low nM potency against 12-LOX, prompted me to examine the selectivity of a few of our top analogs (**35**, **36**, and **37**) against other human LOX isozymes (5-LOX and 15-LOX-2). In addition, we profiled the compounds against cyclooxygenase-1/2 (COX-1/2). As shown in Table 4, we observed no significant inhibition against any of these related enzymes, with exception to **35** which has modest potency (29-fold less active)

towards 15-LOX-1. These results are encouraging because few compounds reported in the literature have achieved both nM potency towards 12-LOX and selectivity against other isozymes.[xxi]

Table 4. Selectivity and Redox Activity of Representative Analogs.[a]

Analog	12-LOX[b]	15-LOX-1[b]	15-LOX-2[b]	5-LOX[b]	COX-1/2[c]	Redox Activity[d]
35	0.34	9.8	>100	> 100	NI	NI
36	0.79	>100	>100	>100	NI	NT
37	0.57	>100	>100	>35	NI	NT

[a] Selectivity profiling of **35** and other top compounds. [b]IC_{50} values are reported in μM. The error for these values are below 20%.. [c] Compounds were tested at 15 μM and none of the compound exhibited inhibition above 10%. [d]UV-Vis pseudoperoxidase activity assay was performed on **35** and no degradation of the hydroperoxide product was observed at 234 nm, indicating a non-reductive inhibitory mechanism; NI = no inhibition and NT = not tested.

LOX inhibitors are known to exhibit a variety of inhibitory mechanisms; therefore the UV pseudoperoxidase assay is often used to investigate if the inhibition is reductive in nature.[xxv] I performed the assay on **35** and **36** with 12-LOX and no degradation of the hydroperoxide product was observed at 234 nm, indicating a non-reductive inhibitory mechanism (Table 4). To investigate the inhibition mechanism further, I performed steady-state kinetics using both **35** and **36** by monitoring the formation of 12-HPETE as a function of substrate and inhibitor concentration in the presence of 0.01% Triton X-100. Replots of K_m/V_{max} and $1/V_{max}$ versus inhibitor concentration yielded linear trends for both **35** and **36**. The K_i for **35** equaled 0.35 +/- 0.08 mM and 0.53 +/- 0.2 mM for **36**, from the K_m/V_{max} graphs.
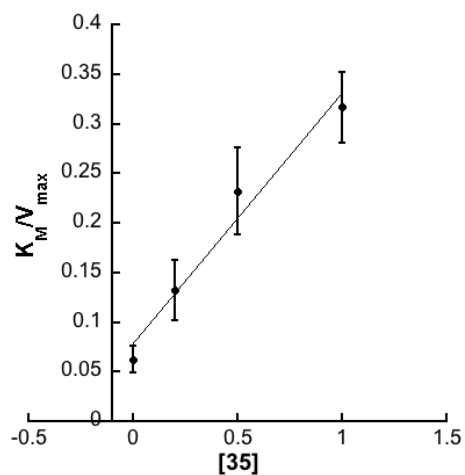
Figure 2. Steady-state kinetics data for the determination of K_i for 12-LOX with **35**. K_M/V_{max} (x-intercept, K_M/V_{max} units are mM/mmol/min/mg) versus [Inhibitor] (μM) is the secondary replot of the inhibition data, which yielded a K_i of 0.35 +/- 0.08 mM.
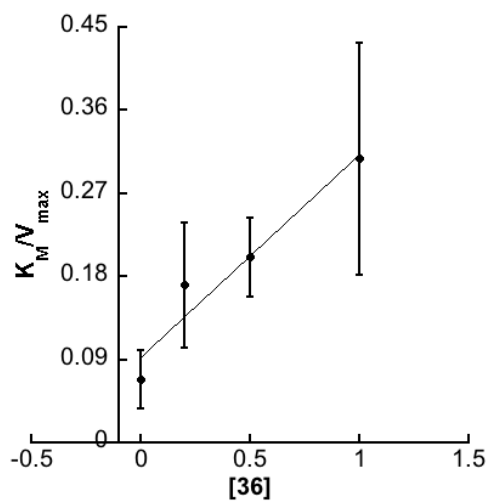

Figure 3. Steady-state kinetics data for the determination of K_i for 12-LOX with **36**. K_M/V_{max} (x-intercept, K_M/V_{max} units are mM/mmol/min/mg) versus [Inhibitor] (μM) is the secondary replot of the inhibition data, which yielded a K_i of 0.53 +/- 0.2 mM.

The K_i' equaled 0.72 +/- 0.1 mM for **35** and 0.62 +/- 0.1 mM for **36**, from the $1/V_{max}$

graphs.

Figure 4. Steady-state kinetics data for the determination of K_i' for 12-LOX with **35**. $1/V_{max}$ (y-intercept, $1/V_{max}$ units are 1/mmol/min/mg) versus [Inhibitor] (µM) is the secondary replot of the inhibition data, which yielded a K_i of 0.72 +/- 0.1 mM.
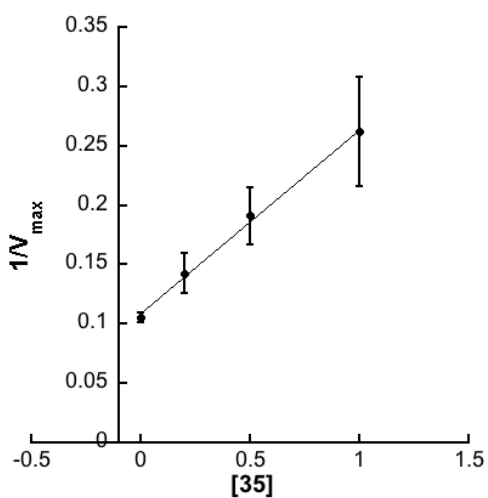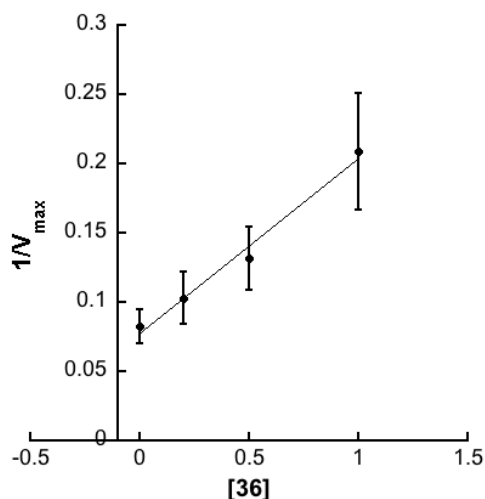
Figure 5. Steady-state kinetics data for the determination of $K_i^{'}$ for 12-LOX with **36**. $1/V_{max}$ (y-intercept, $1/V_{max}$ units are 1/mmol/min/mg) versus [Inhibitor] (μM) is the secondary replot of the inhibition data, which yielded a K_i of 0.63 +/- 0.1 mM.

The data for both **35** and **36** correlate with their IC_{50} values (Table 2) and indicate that both molecules are mixed inhibitors, which is a common property of both 12-LOX[xxi] and 15-LOX-1[xxvi] inhibitors in general.

Upon completion of the SAR campaign, we then sought to explore the activity of **35** in relevant cell-based systems. As noted previously, 12-LOX has been linked to platelet activation, which plays a central role in the regulation of primary hemostasis and arterial thrombosis. Consequently, failure to attenuate platelet activation results in excessive clot formation leading to adverse cardiovascular events such as myocardial infarction and stroke. Previous studies have shown that 12-LOX in human platelets is highly activated following stimulation of the protease-activated receptor-4 (PAR4) by

the PAR4-activating peptide (PAR4-AP).[xxvii] Moreover, the bioactive metabolite of 12-LOX (12-HETE), resulting from the stereospecific oxidation of AA and reduction by peroxidases, demonstrates pro-thrombotic effects in human platelets.[xxviii] Therefore, treatment of PAR4-AP-induced human platelets with a small molecule 12-LOX inhibitor should attenuate the platelet aggregation in a dose-dependent manner. The results from the Holinstat Laboratory in Figure 2B show that **35** does in fact significantly reduce PAR4-AP induced platelet aggregation. Further, 12-LOX has been shown to play a role in calcium mobilization in human platelets and inhibition of 12-LOX should lead to a reduced concentration of free calcium in the platelet.[xxix] To study this, we stimulated human platelets with 200 μM PAR4-AP and measured the free calcium in the platelet, using a C6 Accuri flow cytometer with various concentrations of **35** (Figure 2A). These data demonstrate that at concentrations as low as 250 nM of **35** calcium mobilization is reduced significantly (measured as fold change), with complete inhibition of calcium mobilization occurring at ~5 μM. Comparable results were obtained with another top active (compound **36)** and are shown in Figure 6.
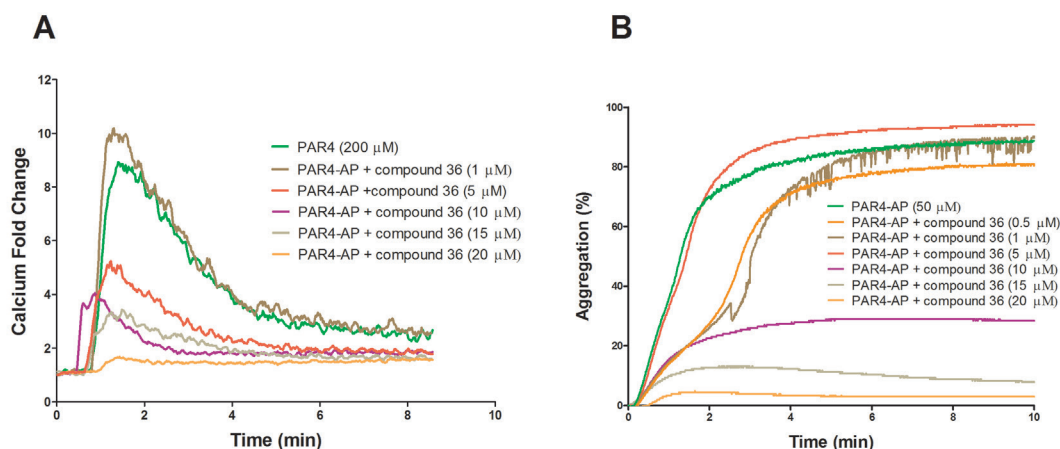
Figure 6. PAR4-AP-induced calcium mobilization (A) and platelet aggregation (B) in human platelets. For A: Washed human platelets (1×10^6 platelets/mL) were stimulated with 200 μM PAR4-AP in the absence or presence of increasing concentrations of compound **36**. Calcium mobilization was decreased as the concentration of compound **36** was increased. Calcium was measured in real time using a C6 Accuri flow cytometer. The experiments were done in triplicate. For B: Platelet aggregation of human platelets (3×10^8 platelets/mL) was measured in real-time using a Chronolog Lumi-Aggregometer (model 700D) following addition of PAR4-AP.
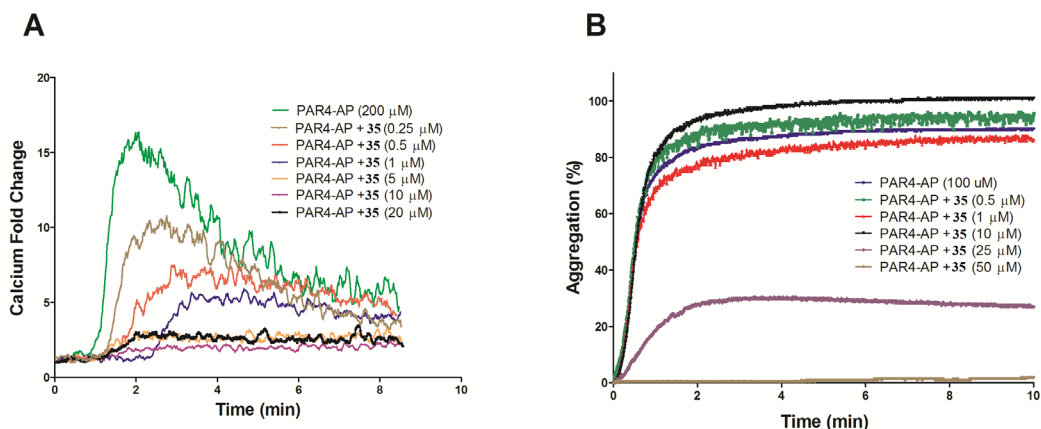

Figure 7. PAR4-AP-induced calcium mobilization (A) and platelet aggregation (B) in human platelets. For A: Washed human platelets (1×10^6 platelets/mL) were stimulated with 200 μM PAR4-AP in the absence or presence of increasing concentrations of **35**. Calcium mobilization was decreased as the concentration of **35** was increased. Calcium was measured in real time using a C6 Accuri flow cytometer. The experiments were done in triplicate. For B: Platelet aggregation of human platelets (3×10^8 platelets/mL) was measured in real-time using a Chronolog Lumi-

Aggregometer (model 700D) following addition of PAR4-AP. While 10 µM **35** did not inhibit platelet aggregation, 25 µM **35** inhibited 80% platelet aggregation in washed human platelets.

To further validate these compounds, the Nadler laboratory then assessed the ability of **35** to inhibit 12-LOX in cell-based models relevant for diabetic disease. As discussed above, 12-LOX is expressed in pancreatic β cells and its metabolic product, 12-HETE, is implicated in cytokine-induced cell death. Specifically, 12(*S*)-HETE has been shown to reduce metabolic activity inhibit insulin secretion and ultimately induce cell death in human islets.[xxx] Towards this end, the Nader laboratory tested **35** in both a mouse derived β-cell line (BTC3) and human primary donor islets to determine its ability to inhibit AA/calcium ionophore induced stimulation of 12-HETE. **35** was able to potently inhibit 12-HETE in BTC3 cells with an approximate IC_{50} of 1 µM, as measured by ELISA (Figure 3A). Given the difficulty in obtaining primary human islets from donated tissues, the activity in human islets was performed at a single concentration. The data presented in Figure 3B demonstrates significant inhibition of AA/IONO-induced 12-HETE production, at 10 µM of **35**.
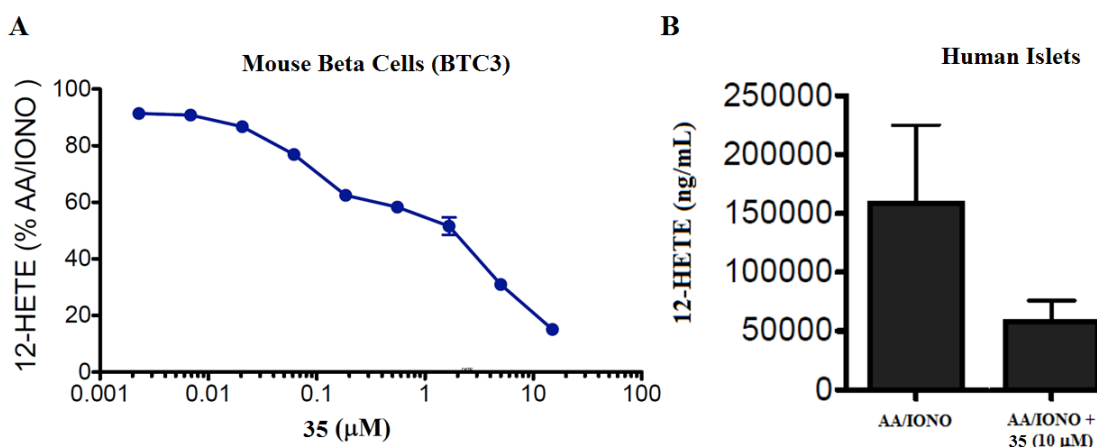
Figure 8. Inhibition of 12-HETE in mouse beta cells (A) and human islets (B). For A: Mouse beta cells (BTC3) were treated with   arachidonic acid and calcium ionophore (AA/IONO) alone or in the presence of **35**. Graphed are the levels of 12-HETE expressed as a percentage of that detected in cells stimulated with AA/IONO alone. For B: The graph represents the increase (above control/unstimulated) in 12-HETE for human primary donor islets stimulated with arachidonic acid and calcium ionophore (AA/IONO) alone or in the presence of 10 μM of **35**. 12-HETE was measured by ELISA.

While the above data demonstrates activity in disease relevant cell-based models, in order to validate the potential use of **35** in proof of concept animal models, we needed to determine both its *in vitro* ADME and *in vivo* PK properties. These data were performed by a contracted laboratory and are summarized in Tables 5 and 6 respectively. Compound **35** demonstrated excellent microsomal stability with both rat ($T_{1/2}$ >30 minutes) and mouse ($T_{1/2}$ >300 minutes) and was found to be stable to mouse plasma over a 2 hour period (100% remaining). Moreover, **35** showed no degradation in various aqueous buffers (pH 2-9) and was stable to 5 mM glutathione suggesting excellent stability. One remaining liability is its aqueous solubility, which is <5 μM, however improved solubility is observed in the assay buffer (qualitative analysis). Moreover, we recently found that benzoxazole derivative (**36**) has much improved solubility in buffer (>10-fold) albeit with slightly weaker potency towards 12-LOX. As a result, we plan to investigate in more detail the ADME/PK properties of compound **36** in future studies.

Compound	PBS buffer (pH 7.4) Solubility (μM)	Microsomal Stability T$_{1/2}$ (min)[a]		Permeability (10^{-6} cm/s)	Efflux ratio	Mouse Plasma Stability remaining at 2 hours	PBS buffer (pH 7.4) Stability at 48 h
35	<5	>30 (rat)	>300[a] (mouse)	1.5 (A→B)[a]	1.8	100%[a]	100%

Table 5. *in vitro* ADME profile for **35**. Experiments were conducted at Pharmaron Inc.[a] represents the stability in the presence of NADPH. **35** showed no degradation without NADPH present over a 1 h period.

Compound	Route[a]	T$_{1/2}$ (h)	T$_{max}$ (h)	C$_{max}$ (μM)	AUC$_{inf}$ (μM)	V$_d$ (L/kg)	Cl (mL/min/kg)	%F	MRT[b]
35	IV	3.4	NA	112	34	0.55	3.4	NA	2.44
	PO	2.9	0.25	38	67	NA	NA	19.8	NA

Table 6. *In vivo* PK (mouse) at 3 mpk (IV) and 30 mpk PO for **35**. All experiments were conducted at Pharmaron Inc. using male CD1 mice (6-8 weeks of age). Data was collected in triplicate at 8 time points over a 24 h period. [a]Formulated as a solution (5% DMSO, 10% Solutol, 20% PEG400, 65% water). [b] represents the time for elimination of 63.2% of the IV dose.

Compound **35** showed moderate cell permeability in the Caco-2 assay (1.5 x 10^{-6}

cm/s) and does not appear to be a substrate for Pgp given the efflux ratio of <2. With

this data in hand, we then sought to explore the *in vivo* PK (mouse) properties of the molecule (Table 6). Exploratory formulation studies led to an appropriate vehicle (DMSO:Solutol:PEG400:water; 5/10/20/65 v/v/v/v) in which **35** was administered as a solution via IV (3 mpk) and PO (30 mpk). These studies demonstrate that **35** is orally bioavailable (%F = ~20), with a moderate half-life ($T_{1/2}$ = 2.9 hours). At 30 mpk dosing, **35** achieves a C_{max} of over 135 times the *in vitro* IC_{50} and remains over IC_{50} value for over 12 hours. The compound has low clearance (3.4 mL/min/kg) and good overall exposure (AUC_{inf}) of 38 μM. The volume of distribution (V_d) is (0.55 L/kg) which is low but suggests a reasonable distribution between tissue and blood. Given the favorable microsomal stability (phase I metabolism) yet modest *in vivo* $T_{1/2}$ we suspected that the phenolic moiety could be glucuronidated (phase II metabolism) leading to higher clearance than anticipated. In fact, incubation with UDPGA co-factor instead of NADPH led to a $T_{1/2}$ of ~8 minutes (vs. >30 minutes with NADPH). We thought that the sterically hindered environment of the 2-OH would possibly prevent glucuronidation from occurring, yet this data suggests otherwise. Another strategy which has been used to obviate a glucuronidation liability is to introduce electron-withdrawing groups next to the phenolic moiety of interest.[xxxi] As such, we employed this strategy with the synthesis of analog **71** (2-OH, 3-Cl), however, this did not change the rate of glucuronidation. In addition to introducing other electron-withdrawing groups to the ring, another approach is to modify the phenolic hydroxyl using a pro-drug approach. Ideally, the pro-drug would be slowly hydrolyzed to the free phenol, after it has bypassed first-pass metabolism. This approach has been used

successfully in several marketed drugs, which contain phenolic groups.[xxxii] We plan to investigate these various approaches in future studies.

As stated above, previously reported inhibitors of 12-LOX, such as baicalein and nor-dihydroguairetic acid (NDGA), "bromo-phenols" or "pyrazole derivatives" (see Figure 1) all possess several liabilities. These compounds are not only less potent and less selective, but are also not easily amenable to further optimization. Our previously described 12-LOX inhibitor (**ML127,** Figure 1) does demonstrate potent inhibition (<500 nM) and excellent selectivity but was found to exhibit flat SAR thus providing little opportunity for further modification. In this work we describe a new chemotype that is structurally distinct from all previously reported inhibitors, and possesses a drug-like scaffold. Compound **35**, and related top analogs demonstrate potent (<500 nM) inhibition towards 12-LOX and excellent selectivity against related enzymes (15-LOX-1, 5-LOX, 15-LOX-2, COX 1/2). This series is readily amenable to structural modifications and displays clear and tractable SAR. Compound **35** exhibits a favorable *in vitro* ADME and *in vivo* PK profile with activity in disease relevant cell-based systems, such thrombosis (platelet aggregation and calcium mobilization) and diabetes (12-HETE reducing in β-cells). Future studies are aimed at additional biological characterization of other top compounds (e.g. **36**, **37** and **67**), which possess comparable potency to **35** but with improved selectivity and solubility (e.g. **36**). We hope these compounds have the potential to further validate 12-LOX as a potential therapeutic target for a variety of diseases and we make them readily available to the research community.

EXPERIMENTAL SECTION:

All air or moisture sensitive reactions were performed under positive pressure of

nitrogen with oven-dried glassware. Chemical reagents and anhydrous solvents were

obtained from commercial sources and used as-is. Preparative purification was

performed on a Waters semi-preparative HPLC. The column used was a Phenomenex

Luna C18 (5 micron, 30 x 75 mm) at a flow rate of 45 mL/min. The mobile phase

consisted of acetonitrile and water (each containing 0.1% trifluoroacetic acid). A

gradient of 10% to 50% acetonitrile over 8 minutes was used during the purification.

Fraction collection was triggered by UV detection (220 nm). Analytical analysis for

purity was determined by two different methods denoted as Final QC Methods 1 and

2. Method 1: Analysis was performed on an Agilent 1290 Infinity Series HPLC.

UHPLC Long Gradient Equivalent 4% to 100% acetonitrile (0.05% trifluoroacetic

acid) in water over 3.5 minutes run time of 4 minutes with a flow rate of 0.8 mL/min.

A Phenomenex Kinetex 1.7 micron C18 column (2.1 x 100 mm) was used at a

temperature of 50 °C. Method 2: analysis was performed on an Agilent 1260 with a 7

minute gradient of 4% to 100% acetonitrile (containing 0.025% trifluoroacetic acid)

in water (containing 0.05% trifluoroacetic acid) over 8 minute run time at a flow rate

of 1 mL/min. A Phenomenex Luna C18 column (3 micron, 3 x 75 mm) was used at a

temperature of 50 °C. Purity determination was performed using an Agilent Diode

Array Detector for both Method 1 and Method 2. Mass determination was performed

using an Agilent 6130 mass spectrometer with electrospray ionization in the positive

mode. All of the analogs for assay have purity greater than 95% based on both

analytical methods. ^{1}H and ^{13}C NMR spectra were recorded on a Varian 400 (100) MHz spectrometer. High resolution mass spectrometry was recorded on Agilent 6210 Time-of-Flight LC/MS system.

Methods.

General Synthetic Procedures Performed at the NIH. (Scheme 1, Method A): 4-amino-*N*-(thiazol-2-yl)benzene sulfonamide (0.39 mmol) (**2**), and the required benzaldehyde (0.67 mmol) was added to a microwave vial and ethanol (2 mL) was added. The reaction vessel was sealed and heated to 100 ºC for 4-18 h. The reaction mixture was allowed to cool to room temperature and sodium borohydride (0.80 mmol) was added, stirred for 30 min, during which time the reaction turned clear and then cloudy. The resulting solids were filtered, washed with ethanol, and purified using a prep-HPLC (gradient 10-100% acetonitrile w/ 0.1% TFA in water w/ 0.1% TFA) to give the desired product.

(Scheme 1, Method B) A solution of 4-bromo-*N*-(thiazol-2-yl)benzene sulfonamide (0.31 mmol) (**3**) in dioxane (1 mL) was added to a mixture of sodium tert-butoxide (0.78 mmol), 4,5-bis(diphenylphosphino)-9,9-dimethylxanthene (Xantphos) (0.02 mmol) and tris(dibenzylideneacetone)dipalladium(0) (Pd$_2$dba$_3$) (6.27 µmol) in dioxane (1 mL). The resulting mixture was degassed with argon for 15 min. Then the requisite benzylamine (0.38 mmol) was added, the vessel was sealed and heated to 100 °C for 30 min in Biotage® microwave reactor. The reaction mixture was cooled to room temperature and filtered through celite. Silicycle® silica bound thiol was

added and stirred overnight, again filtered through a pad of celite, concentrated, and

purified by prep-HPLC (gradient 10-100% acetonitrile w/ 0.1% TFA in water w/

0.1% TFA) to give the desired product.

(Scheme 1, Method C) 4-aminobenzenesulfonamide (**4**) (1.00 g, 5.81 mmol), 2-

hydroxy-3-methoxybenzaldehyde (1.00 g, 7.00 mmol) in EtOH (29 mL) was heated

to reflux for 6 h until reaction is an orange turbid mixture. The reaction mixture was

cooled to room temperature before sodium borohydride (0.33 g, 8.71 mmol) was

added and stirred for an additional 30 min. A white solid forms after 30 min and is

collected by filtration and washed with copious amounts of ethanol, dried under

vacuum and used as is in subsequent reactions. ^{1}H NMR (400 MHz, DMSO-d_6) δ

7.60–7.27 (m, 2H), 6.75–6.40 (m, 4H), 6.06 (t, J = 7.63 Hz, 1H), 4.18 (s, 2H), and

3.65 (s, 3H); ^{13}C NMR (101 MHz, DMSO) δ 40.37, 55.32, 108.91, 109.42, 109.55,

111.29, 111.40, 121.05, 125.05, 127.49, 129.92, 150.17, 152.36, and 156.94; LC-MS

retention time (Method 1): 2.876 min. General procedure: (**Step iv**) 4-(2-hydroxy-3-

methoxybenzylamino)benzenesulfonamide (**5**) (0.58 mmol), arylbromide (0.70

mmol), K_2CO_3 (1.45 mmol), N,N'-dimethylethylenediamine (0.29 mmol), and

copper(I)iodide (0.03 mmol) in 1,4-dioxane (1.5 mL) were place under N_2 and sealed

in a 5 mL sealed tube. The reaction was heated to 80 °C for 6 to 8 h and monitored by

LC/MS analysis. Upon completion the heterogeneous mixture was cooled to room

temperature, filtered, and washed with dioxane. The solution was passed through a

thiol cartridge (metal scavenging), diluted with AcOEt and washed with NH_4Cl (2X),

water, and brine. The crude material was purified using a prep-HPLC (gradient 10-100% acetonitrile w/ 0.1% TFA in water w/ 0.1% TFA) to give the desired product.

(Scheme 1, Method D: *Representative Example*) **N-(benzo[d]thiazol-2-yl)-4-nitrobenzenesulfonamide (7): (Step V)** To a stirred solution of benzo[d]thiazol-2-amine (0.50 g, 3.35 mmol) in pyridine (1.60 mL, 20.08 mmol) was added 4-nitrobenzene sulfonyl chloride (**6**) (0.82 g, 3.68 mmol) in three equal parts. The reaction mixture was heated for 75 min at 100 °C, cooled to room temperature, after which time a yellow precipitate formed. The reaction mixture was allowed to sit at room temperature for 2 h then the yellow solid was collected by filtration, washed with ethanol, and dried under reduced pressure overnight to give 1.10 g of the desired product **7**. ^{1}H NMR (400 MHz, DMSO-d_6) δ 8.90 (ddt, J = 0.75, 1.63, and 5.59 Hz, 1H), 8.54, 8.41–8.28 (m, 1H), 8.13–7.96 (m, 2H), 7.82 (dq, J = 0.80, and 7.96 Hz, 1H), 7.45–7.34 (m, 1H), 7.31–7.19 (m, 1H); LC-MS retention time (Method 1): 3.272 min; HRMS: m/z (M+H)$^{+}$ = (Calculated for $C_{13}H_{10}N_3O_4S_2$, 336.0107) found 336.0107.

4-amino-*N*-(benzo[d]thiazol-2-yl)benzenesulfonamide: (Step VI) N-(benzo[d]thiazol-2-yl)-4-nitrobenzenesulfonamide (0.20 g, 0.60 mmol), zinc (0.16 g, 2.39 mmol), acetic acid (0.14 mL, 2.39 mmol) was dissolved in MeOH (3 mL), and the mixture heated to 60 °C for 2 h. The heterogeneous mixture was filtered through a pad of celite washed with hot methanol, concentrated and purified using prep-HPLC (gradient 10-100% acetonitrile w/ 0.1% NH$_4$OH in water w/ 0.1% NH$_4$OH) to give

the desired product. Alternate nitro reduction: *N*-(benzo[d]thiazol-2-yl)-4-nitrobenzenesulfonamide was dissolved in MeOH/EtOAc/THF (1:1:1) to give a 0.05 M solution passed through the H-Cube Pro® flow reactor using a 10% Pd/C, 70 mm CatCart® at 50 bar and 50 °C for two cycles at 0.9 mL/min. The solution was concentrated to give a pale yellow solid in a quantitative yield. ^{1}H NMR (400 MHz, DMSO-d_6) δ 7.49–7.34 (m, 3H), 7.18 (ddd, *J* = 0.56, 1.21, and 8.00 Hz, 1H), 7.03 (ddd, *J* = 1.33, 7.24, and 7.97 Hz, 1H), 6.83 (ddd, *J* = 1.20, 7.25, and 7.68 Hz, 1H), 6.51–6.38 (m, 2H), 5.42 (s, 2H); LC-MS retention time (Method 2): 3.933 min; HRMS: *m/z* (M+H)$^+$ = (Calculated for $C_{13}H_{12}N_3O_2S_2$, 306.0365) found 306.0360.

_N_-(benzo[d]thiazol-2-yl)-4-((2-hydroxy-3-methoxybenzyl)amino)benzenesulfonamide (Step VII, representative example) **(35, ML355):** 4-amino-N-(benzo[d]thiazol-2-yl)benzenesulfonamide (0.10 g, 0.33 mmol), 2-hydroxy-3-methoxybenzaldehyde (0.075 g, 0.491 mmol) were heated in EtOH (1.5 mL) at reflux for 18 h. The reaction mixture was allowed to cool to room temperature before the addition of NaBH$_4$ (0.04 g, 0.98 mmol), and stirred for an additional 6 h. After this time, the reaction mixture was quenched with methanol and water then stirred for 20 min, the solids were filtered through celite, the filtrate collected, and concentrated under reduced pressure to provide a yellow solid. The crude material was purified using a prep-HPLC (gradient 10-100% acetonitrile w/ 0.1% TFA in water w/ 0.1% TFA) to give the desired product **35**. ^{1}H NMR (400 MHz, DMSO-d_6) δ 12.86 (s, 1H), 8.73 (d, *J* = 0.5 Hz, 1H), 7.75 (ddd, *J* = 0.6, 1.2, and 7.9 Hz, 1H), 7.54–7.46 (m, 2H), 7.40–7.31 (m, 1H), 7.28–7.16 (m, 2H), 6.93–6.79 (m, 2H), 6.78–

6.55 (m, 4H), 4.23 (d, J = 5.8 Hz, 2H) and 3.78 (s, 3H); ^{13}C NMR (DMSO-d_6) δ ppm 152.4, 147.7, 144.3, 128.2, 125.7, 122.9, 120.4, 119.0, 111.4, 110.9, 56.2 and 40.6; LC-MS retention time (Method 1): 2.260 min; HRMS: m/z (M+H)$^+$ = (Calculated for $C_{21}H_{19}N_3O_4S_2$, 441.0817) found 441.0819.

Biological Reagents: All commercial fatty acids (Sigma-Aldrich Chemical Company) were re-purified using a Higgins HAIsil Semi-Preparative (5 μm, 250 × 10mm) C-18 column. Solution A was 99.9% MeOH and 0.1% acetic acid; solution B was 99.9% H_2O and 0.1% acetic acid. An isocratic elution of 85% A:15% B was used to purify all fatty acids, which were stored at −80 ºC for a maximum of 6 months.

Human Platelets: Human platelets were obtained from healthy volunteers within the Thomas Jefferson University community and the Philadelphia area. These studies were approved by the Thomas Jefferson University Institutional Review Board, and informed consent was obtained from all donors before blood draw. Blood was centrifuged at 200 g for 13 min at room temperature. Platelet-rich plasma was transferred into a conical tube containing a 10% acid citrate dextrose solution (39 mM citric acid, 75 mM sodium citrate, and 135 mM glucose, pH 7.4) and centrifuged at 2000 g for 15 min at room temperature. Platelets were resuspended in Tyrode's buffer (12 mM NaHCO$_3$, 127 mM NaCl, 5 mM KCl, 0.5 mM NaH$_2$PO$_4$, 1 mM MgCl$_2$, 5 mM glucose, and 10 mM HEPES), and the final platelet concentration was adjusted to 3 X 10^8 platelets/mL after counting with a ZI Coulter particle counter (Beckman Coulter, Fullerton, CA). Reported results are the data obtained using platelets from at

least three different subjects. Agonists and inhibitors were used at concentrations indicated in the figures and figure legends.

Over expression and Purification of 12-Human Lipoxygenase, 5-Human Lipoxygenase, 12/15-Mouse Lipoxygenase and the 15-Human Lipoxygenases Performed at UCSC: Human platelet 12-lipoxygenase (12-LOX), human reticulocyte 15-lipoxygenase-1 (15-LOX-1), and human epithelial 15-lipoxygenase-2 (15-LOX-2), were expressed as N-terminally, His_6-tagged proteins and purified to greater than 90% purity, as evaluated by SDS-PAGE analysis.[xxxiii] Human 5-lipoxygenase was expressed as a non-tagged protein and used as a crude ammonium sulfate protein fraction, as published previously.[xxxiv] Iron content of 12-LOX was determined with a Finnigan inductively coupled plasma mass spectrometer (ICP-MS), using cobalt-EDTA as an internal standard. Iron concentrations were compared to standardized iron solutions and used to normalize enzyme concentrations.

High-throughput Screen Materials Performed at NIH: Dimethyl sulfoxide (DMSO) ACS grade was from Fisher, while ferrous ammonium sulfate, Xylenol Orange (XO), sulfuric acid, and Triton X-100 were obtained from Sigma-Aldrich.

12-Lipoxygenase qHTS Assay (AID: 1452) Performed at NIH: All screening operations were performed on a fully integrated robotic system (Kalypsys Inc, San Diego, CA) as described elsewhere.[xxxv] Three μL of enzyme (approximately 80 nM 12-LOX, final concentration) was dispensed into 1536-well Greiner black clear-bottom assay plates. Compounds and controls (23 nL) were transferred via Kalypsys PinTool equipped with 1536-pin array. The plate was incubated for 15 min at room

temperature, and then a 1 µL aliquot of substrate solution (50 µM arachidonic acid

final concentration) was added to start the reaction. The reaction was stopped after

6.5 min by the addition of 4 µL FeXO solution (final concentrations of 200 µM

Xylenol Orange (XO) and 300 µM ferrous ammonium sulfate in 50 mM sulfuric acid).

After a short spin (1000 rpm, 15 sec), the assay plate was incubated at room

temperature for 30 minutes. The absorbances at 405 and 573 nm were recorded using

ViewLux high throughput CCD imager (Perkin-Elmer, Waltham, MA) using standard

absorbance protocol settings. During dispense, enzyme and substrate bottles were

kept submerged into a +4 ºC recirculating chiller bath to minimize degradation. Plates

containing DMSO only (instead of compound solutions) were included approximately

every 50 plates throughout the screen to monitor any systematic trend in the assay

signal associated with reagent dispenser variation or decrease in enzyme specific

activity. Data were normalized to controls, and plate-based data corrections were

applied to filter out background noise.

Lipoxygenase UV-Vis Assay Performed at UCSC: The inhibitor compounds were

screened initially using one concentration point at 25 µM on a Perkin-Elmer Lambda

40 UV/Vis spectrophotometer. The percent inhibition was determined by comparing

the enzyme rates of the control (DMSO solvent) and the inhibitor sample by

following the formation of the conjugated diene product at 234 nm ($\varepsilon = 25,000$ M^{-1}cm^{-1}). The reactions were initiated by adding either of 30 nM 12-LOX, 40 nM 15-

LOX-1, 200 nM 15-LOX-2 or 5-10 µL of 5-LOX crude extract to a cuvette with a 2

mL reaction buffer constantly stirred using a magnetic stir bar at room temperature

(22 ºC). Reaction buffers used for various lipoxygenase were as follows: 25 mM

HEPES (pH 7.3), 0.3 mM $CaCl_2$, 0.1 mM EDTA, 0.2 mM ATP, 0.01% Triton X-100,

10 μM AA for the crude, ammonium sulfate precipitated 5-LOX; and 25 mM HEPES

(pH 7.5), 0.01% Triton X-100, 10 μM AA for 12-LOX, 15-LOX-1 and 15-LOX-2.

The substrate concentration was quantitatively determined by allowing the enzymatic

reaction to go to completion in the presence of 15-LOX-2. For the inhibitors that

showed more than 50% inhibition at the one point screens, IC_{50} values were obtained

by determining the % inhibition, relative to solvent vehicle only, at various inhibitor

concentrations. The data was then plotted against inhibitor concentration, followed by

a hyperbolic saturation curve fit (assuming total enzyme concentration $[E] << K_i^{app}$,

so $IC_{50} \sim K_i^{app}$). It should be noted that all of the potent inhibitors displayed greater

than 80% maximal inhibition, unless stated in the tables. Inhibitors were stored at –

20 °C in DMSO

Steady State Inhibition Kinetics Performed at UCSC: The steady-state kinetics

experiments were performed with **35** to determine the mode of inhibition. The

inhibitor concentrations of 0, 0.2, 0.5 and 1 μM were used. Reactions were initiated

by adding substrate (range 1 – 5 μM AA) to approximately 30 nM 12-LOX in a

constantly stirring 2 mL cuvette containing 25 mM HEPES buffer (pH 7.5), in the

presence of 0.01% Triton X-100. Lipoxygenase rates were determined by monitoring

the formation of the conjugated product, 12-HPETE, at 234 nm ($\varepsilon = 25\ 000\ M^{-1}\ cm^{-1}$)

with a Perkin-Elmer Lambda 45 UV/Vis spectrophotometer. It should be noted that

12-LOX displays higher error in the K_M values at low substrate concentrations (< 1

μM) due to the limits of the spectrophotometer. The substrate concentration was quantitatively determined by allowing the enzymatic reaction to proceed to completion, using 12-LOX or 15-LOX-2. Kinetic data were obtained by recording initial enzymatic rates, at varied substrate and inhibitor concentrations, and subsequently fitted to the Henri-Michaelis-Menten equation, using KaleidaGraph (Synergy) to determine the microscopic rate constants, V_{max} (μmol/min/mg) and V_{max}/K_M (μmol/min/mg/μM). The kinetic rate constants were subsequently replotted with K_M/V_{max} and $1/V_{max}$ versus inhibitor concentration, yielding K_i and $K_i^{'}$, respectively.

Pseudoperoxidase Assay Performed at UCSC: The pseudo-peroxidase activity rates were determined with BWb70c as the positive control, 13-(S)-HPODE as the oxidizing product and 12-LOX or 15-LOX-1 on a Perkin-Elmer Lambda 40 UV/Vis spectrophotometer, as described previously.[xxv] Activity was determined by monitoring the decrease at 234 nm (product degradation) in buffer (50 mM Sodium Phosphate (pH 7.4), 0.3 mM $CaCl_2$, 0.1 mM EDTA, 0.01% Triton X-100, and 20 μM 13-(S)-HPODE). About 60 nM 12-LOX was added to 2 mL buffer containing 20 μM 13-(S)-HPODE, constantly stirred with a rotating stir bar (22 °C). Reaction was initiated by addition of 20 μM inhibitor (1:1 ratio to product). The percent consumption of 13-(S)-HPODE was recorded and loss of product less than 20% was not considered as viable redox activity. Individual controls were conducted consisting of enzyme alone with product and **35** alone with enzyme. These negative controls formed the baseline for the assay, reflecting non-pseudo-peroxidase dependent

hydroperoxide product decomposition. To rule out the auto-inactivation of the enzyme from pseudo-peroxidase cycling, the 12-LOX residual activity was measured after the assay was complete. 20 μM AA was added to the reaction mixture and the residual activity was determined by comparing the initial rates with inhibitor and 13-(*S*)-HPODE versus inhibitor alone, since the inhibitor by itself inherently lowers the rate of the oxygenation. Activity is characterized by direct measurement of the product formation with the increase of absorbance at 234 nm.

Cyclooxygenase assay Performed at UCSC: Roughly 2-5 μg of either COX-1 or COX-2 were added to buffer containing 0.1 M Tris-HCl buffer (pH 8.0), 5 mM EDTA, 2 mM phenol and 1 μM hematin at 37 °C. The selected inhibitors were added to the reaction cell, followed by an incubation of 5 minutes with either of the COX enzymes. The reaction was then initiated by adding 100 μM AA in the reaction cell. Data was collected using a Hansatech DW1 oxygen electrode and the consumption of oxygen was recorded. Indomethasin and the solvent DMSO, were used as positive and negative controls, respectively and the percent inhibition of the enzyme was calculated by comparing the rates from samples and the controls.

Platelet Aggregation Performed at Jefferson University: Washed platelets were adjusted to a final concentration of 3×10^8 platelets/mL. Where indicated, platelets were pretreated with **35** or compound **36** for 10 min at the indicated concentrations for 1 min. The aggregation response to PAR4-AP was measured using an aggregometer with stirring at 1100 RPM at 37 °C.

Calcium Mobilization Performed at Jefferson University: Platelets were

recalcified to a final concentration of 1 mM followed by pre-incubation with Fluo-4

AM for 10 min. The platelets were then treated with **35** or compound **36** for 10 min at

the indicated concentrations before stimulation with the indicated agonist. Calcium

mobilization was measured using the Accuri C6 flow cytometer.

Mouse Beta cells (12-HETE Inhibition) Assay Performed at East Virginia

Medical School: Cells were gown to 90% confluency in 24 well plates in DMEM

(Cat# 11885092, Life Technologies Grand Island, NY) +10% FBS. Cells were pre-

treated with **35** and stimulated as for human islets. After four hours, the media was

removed and spun at 1000 RPM for 5 minutes. The cleared supernatant was stored at

–80 ºC prior to analysis. For analysis, supernatants were extracted on SepPak c18

SPE column (Cat# WAT054945, Waters Corporation, Milford, MA) and dried under

nitrogen gas before reconstitution in 500 μL of 12-HETE ELISA buffer and analysis

following manufacturers recommendations (Cat# 901-050, Enzo Life Sciences,

Plymouth Meeting, PA).

Human Islet (12-HETE Inhibition) Assay Performed at East Virginia Medical

School: Human donor islets obtained from integrated islet distribution program

(www.iidp.coh.org) were incubated overnight in CMRL media (Cat# 15-110-CV

MediaTech, Inc. Manassas, VA) containing 10% Fetal Bovine Serum, 1U penicillin

1 μg streptomycin (pen/strep). Islets were equilibrated in serum free media, (CMRL

containing pen/Strep and 1% fatty acid free human serum albumin (Cat# A1887

Sigma, St. Louis, MO)), for 1 hour prior to pretreatment with 10 µM of **35** for 30 min. For 12-HETE induction, islets were treated with 100 µM arachidonic acid (Cat# BML-FA003-0100, Enzo Life Sciences Plymouth Meeting, PA), and 5 µM A23187 (Cat# C7522, Sigma, St. Louis, MO), for 4 hours at 37 ºC. Islets were harvested, centrifuged at 1000 RPM for 5 minutes with cleared supernatant and islet pellet being stored at -80 ºC. For extraction of the supernatants, samples were acidified to pH 3 with 1N HCl for 30 minutes and spun at 1000 RPM for five minutes. Samples were added to a prepared column (prewashed with 3 mL EtOH, followed by 3 mL of H_2O) and washed with 3 mL H_2O, followed by 3 mL 15% EtOH, and 3 mL Hexane. The samples were eluted with 3 mL of ethyl acetate and dried under nitrogen gas before, reconstitution in 500 mL of 12-HETE ELISA sample buffer (Enzo Life Sciences, Plymouth Meeting, PA). Cell pellets were extracted using $CHCl_3$ / MeOH and samples dried under nitrogen gas before reconstitution in 250 µL of ELISA sample buffer. 12-HETE levels in samples were determined using a 12-HETE ELISA kit (Cat# 901-050, Enzo Life Sciences, Plymouth Meeting, PA).

REFERENCES:

[i] Solomon, E. I.; Zhou, J.; Neese, F.; Pavel, E. G. New insights from spectroscopy into the structure/function relationships of lipoxygenases. *Chem. Biol.* **1997**, *4*, 795–808. (b) Brash, A. R. Lipoxygenases: Occurrence, Functions, Catalysis and Acquisition of Substrate. *J. Biol. Chem*. **1999**, *274*, 23679–23682.

[ii] Serhan, C. N.; Petasis, N. A. Resolvins and Protectins in Inflammation Resolution. *Chem*. *Rev*. **2011**, *111*, 5922-5943.

[iii] (a) Ghosh, J. Inhibition of Arachidonate 5-Lipoxygenase Triggers Prostate Cancer Cell Death through Rapid Activation of C-Jun N-Terminal Kinase. *Biochem. Biophys.*

Res. Commun. **2003**, *307*, 342-349. (b) Ghosh, J., Myers, C. E. Inhibition of Arachidonate 5-Lipoxygenase Triggers Massive Apoptosis in Human Prostate Cancer Cells. *Proc. Natl. Acad. Sci. U. S. A.* **1998,** *95*, 13182-13187. (c) Nakano, H., Inoue, T., Kawasaki, N., Miyataka, H., Matsumoto, H., Taguchi, T., Inagaki, N., Nagai, H., Satoh, T. Synthesis and Biological Activities of Novel Antiallergic Agents with 5-Lipoxygenase Inhibiting Action. *Bioorg. Med. Chem.* **2000**, *8*, 373-280.

[iv] Radmark, O., Samuelsson, B. 5-Lipoxygenase: Regulation and Possible Involvement in Atherosclerosis. *Prostaglandins Other Lipid Mediat.* **2007**, *83*, 162-174.

[v] Berger, W.; De Chandt, M. T.; Cairns, C. B. Zileuton: Clinical Implications of 5-Lipoxygenase Inhibition in Severe Airway Disease. *Int. J. Clin. Pract.* **2007**, 61, 663–676.

[vi] (a) Cyrus, T.; Witztum, J. L.; Rader, D. J.; Tangirala, R.; Fazio, S.; Linton, M. F.; Funk, C.D. Disruption of the 12/15-lipoxygenase gene diminishes atherosclerosis in apo E–deficient mice *J. Clin. Invest.* **1999,** *103*, 1597-1604. (b) Harats, D.; Shaish, A.; George, J.; Mulkins, M.; Kurihara, H.; Levkovitz, H.; Sigal, E. Overexpression of 15-lipoxygenase in vascular endothelium accelerates early atherosclerosis in LDL receptor-deficient mice. *Arteriosler. Thromb. Vasc. Biol.* **2000**, *20*, 2100-2105.

[vii] Pratico, D.; Zhukareva, V.; Yao, Y.; Uryu, K.; Funk, C. D.; Lawson, J. A.; Trojanowski, J. Q.; Lee, V. M. 12/15-Lipoxygenase is increased in Alzheimer's

disease: possible involvement in brain oxidative stress. *Am. J. Pathol.* **2004**, *164*, 1655-1662.

[viii] (a) van Leyen, K.; Arai, K.; Jin, G.; Kenyon, V.; Gerstner, B.; Rosenberg, P. A.; Holman, T. R.; Lo, E. H. Novel lipoxygenase inhibitors as neuroprotective reagents. *J. Neurosci. Res*. **2008**, *86*, 904-909. (b) van Leyen, K.; Kim, H. Y.; Lee, S. R.; Jin, G.; Arai, K.; Lo, E. H. Baicalein and 12/15-lipoxygenase in the ischemic brain. *Stroke.* **2006**, *37*, 3014-3018.

[ix] Yamamoto, S. Mammalian lipoxygenases: Molecular Structures and functions. *Biochim. Biophys. Acta.* **1992**, *1128*, 117-131. (b) Funk, C.D.; Keeney, D.S.; Oliw, E. H.; Vogel, S.; Muller-Decker, K.; Mincheva, A.; Lichter, P.; Marks, F.; Krieg, P. Murine epidermal lipoxygenase (Aloxe) encodes a 12-lipoxygenase isoform. *FEBS Lett.* **1997**, *402*, 162-166.

[x] (a) Catalano, A.; Procopio, A. New aspects on the role of lipoxygenases in cancer progression. *Histol. Histopathol.* **2005,** *20*, 969-975. (b) Nie, D.; Hillman, G. G.; Geddes, T.; Tang, K.; Pierson, C.; Grignon, D. J.; Honn, K.V. Platelet-type 12-lipoxygenase in a human prostate carcinoma stimulates angiogenesis and tumor growth. *Cancer Res*. **1998**, *58*, 4047–4051. (c) Natarajan, R.; Esworthy, R.; Bai, W.; Gu, J. L.; Wilczynski, S.; Nadler, J. L. Increase 12-lipoxygenase expression in breast cancer cells and tissues. Regulation by epidermal growth factor. *J. Clin. Endocrinol. Metab*. **1997,** *82*, 1790–1798. (d) Kamitani, H.; Geller, M.; Eling, T. The possible

involvement of 15-lipoxygenase/leukocyte type 12-lipoxygenase in colorectal carcinogenesis. *Adv. Exp. Med. Biol*. **1999**, *469*, 593–598. (e) Soriano, A. F.; Helfrich, B.; Chan, D. C.; Heasley, L. E.; Bunn, P. A.; Chou, T. C. Synergistic effects of new chemopreventive agents and conventional cytotoxic agents against human lung cancer cell lines. *Cancer Res*. **1999**, *59*, 6178–6184.

[xi] (a) *Nappez, C.; Liagre, B.; Beneytout, J. L. Changes in lipoxygenase activities in human erythroleukemia (HEL) cells during diosgenin-induced differentiation. Cancer Lett*. **1995***, 96,* 133–*140.* (b) *Timár, J.; Silletti, S.; Bazaz, R.; Raz, A.; Honn, K.V. Regulation of melanoma-cell motility by the lipoxygenase metabolite 12-(S)-HETE. Int. J. Cancer,* **1993***, 55,* 1003–*1010.* (c) *Honn, K.V.; Timár, J.; Rozhin, J.; Bazaz, R.; Sameni, M.; Ziegler, G.; Sloane, B. A lipoxygenase metabolite, 12-(S)-HETE, stimulates protein kinase C-mediated release of cathepsin B from malignant cells. Exp. Cell. Res*. **1994***, 214,* 120–*130.* (d) *Nie, D.; Tang, K.; Diglio, C.; Honn, K. Eicosanoid regulation of angiogenesis: role of endothelial arachidonate 12-lipoxygenase. Blood* **2000***, 95,* 2304–*2311.*

[xii] (a) McDuffie, M.; Maybee, N. A.; Keller, S. R.; Stevens, B. K.; Garmey, J. C.; Morris, M. A.; Kropf, E.; Rival, C.; Ma, K.; Carter, J. D. Tersey, S. A.; Nunemaker, C. S.; Nadler, J. L. Nonobese diabetic (NOD) mice congenic for a targeted deletion of 12/15-Lipoxygenase are protected from autoimmune diabetes. *Diabetes* **2008**, *57*, 199-209. (b) Bleich, D.; Chen, S.; Zipser, B.; Sun, D.; Funk, C. D.; Nadler, J. L. Resistance to type 1 diabetes induction in 12-lipoxygenase knockout mice. *J. Clin.*

Invest. **1999**, *103*, 1431-1436. (c) Imai, Y.; Dobrian, A. D.; Weaver, J. R.; Butcher, M. J.; Cole, B. K.; Galkina, E. V.; Morris, M. A.; Taylor-Fishwick, D. A.; Nadler, J. L. Interaction between cytokines and inflammatory cells in islet dysfunction, insulin resistance and vascular disease. *Diabetes Obes. Metab.* **2013**, *15* (Suppl. 3), 117-129. (d) Ma, K.; Nunemaker, C. S.; Wu, R.; Chakrabarti, S. K.; Taylor-Fishwick, D. A.; Nadler, J. L. 12-Lipoxygenase Products Reduce Insulin Secretion and β-cell Viability in Human Islets. *J. Clin. Endocrinol. Metab.* **2010**, *95*, 887-893.

[xiii] Chen, M.; Yang, Z. D.; Smith, K. M.; Carter, J. D.; Nadler, J. L. Activation of 12-Lipoxygenase in proinflammatory cytokine-mediated β-cell toxicity. *Diabetologia* **2005**, *48*, 486-495.

[xiv] (a) Brash, A. R. A review of possible roles of the platelet 12-lipoxygenase. *Circulation* **1985**, *72*, 702-707.

[xv] (a) Aharony, D.; Smith, J. B.; Silver, M. J. Regulation of arachidonate-induced platelet aggregation by the lipoxygenase product, 12-hydroperoxyeicosatetraenoic acid. *Biochim. Biophys. Acta* **1982**, *718*, 193-200. (b) Chang, J.; Blazek, E.; Kreft, A. F.; Lewis, A. J. Inhibition of platelet and neutrophil phospholipase A2 by hydroxyeicosatetraenoic acids (HETES). A novel pharmacological mechanism for regulating free fatty acid release. *Biochem. Pharmacol.* **1985**, *34*, 1571-1575. (c) Nyby, M. D.; Sasaki, M.; Ideguchi, Y.; Wynne, H. E.; Hori, M. T.; Berger, M. E.; Golub, M. S.; Brickman, A. S.; Tuck, M. L. Platelet lipoxygenase inhibitors attenuate

thrombin-and thromboxane mimetic-induced intracellular calcium mobilization and platelet aggregation. *J. Pharmacol. Exp. Ther.* **1996**, *278*, 503-509.

[xvi] Yeung, J.; Apopa, P. L.; Vesci, J.; Kenyon, V.; Rai, G.; Jadhav, A.; Simeonov, A.; Holman, T. R.; Maloney, D. J.; Boutaud, O.; Holinstat. Protein Kinase C Regulation of 12-Lipoxygenase-Mediated Human Platelet Activation. *Mol. Pharmacol.* **2012**, *81*, 420-430.

[xvii] (a) Whitman, S.; Gezginci, M.; Timmermann, B. N.; Holman, T. R. Structure-activity relationship studies of nordihydroguaiaretic acid inhibitors toward soybean, 12-human, and 15-human lipoxygenase. *J. Med. Chem.* **2002**, *45*, 2659–2661. (b) Deschamps, J. D.; Kenyon, V. A.; Holman, T. R. Baicalein is a potent in vitro inhibitor against both reticulocyte 15-human and platelet 12-human lipoxygenases. *Bioorg. Med. Chem.* **2006**, *14*, 4295–4301. (c) Segraves, E. N.; Shah, R. R.; Segraves, N. L.; Johnson, T. A.; Whitman, S.; Sui, J. K.; Kenyon, V. A.; Cichewicz, R. H.; Crews, P.; Holman, T. R. Probing the activity differences of simple and complex brominated aryl compounds against 15-soybean, 15-human, and 12-human lipoxygenase. *J. Med. Chem.* **2004**, *47*, 4060–4065. (d) Amagata, T.; Whitman, S.; Johnson, T.; Stessmann, C. C.; Carroll, J.; Loo, C.; Clardy, J.; Lobkovsky, E.; Crews, P.; Holman, T. R. Sponge Derived Terpenoids with Selectivity towards Human 15-Lipoxygenase versus Human 12-Lipoxygenase. *J. Nat. Prod.* **2003**, *66*, 230–235. (e) Cichewicz, R. H.; Kenyon, V. A.; Whitman, S.; Morales, N. M.; Arguello, J. F.; Holman, T. R.; Crews, P. Redox inactivation of human 15-lipoxygenase by marine-

derived meroditerpenes and synthetic chromanes: archetypes for a unique class of selective and recyclable inhibitors. *J. Am. Chem. Soc.* **2004**, *126*, 14910–14920. (f) Vasquez-Martinez, Y.; Ohri, R. V.; Kenyon, V.; Holman, T. R.; Sepulveda-Boza, S. Structure-activity relationship studies of flavonoids as potent inhibitors of human platelet 12-hLO, reticulocyte 15-hLO-1, and prostate epithelial 15-hLO-2. *Bioorg. Med. Chem.* **2007**, *15*, 7408–7425.

[xviii] (a) Sailer, E. R.; Schweizer, S.; Boden, S. E.; Ammon, H. P. T.; Safayhi, H. Characterization of an acetyl-11-keto-B-boswellic acid and arachidonate-binding regulatory site of 5-lipoxygenase using photoaffinity labeling. *Eur. J. Biochem.* **1998**, *256*, 364–368. (b) Malterud, K. E.; Rydland, K. M. Inhibitors of 15-lipoxygenase from orange peel. *J. Agric. Food Chem.* **2000**, *48*, 5576–5580. (c) Moreau, R. A.; Agnew, J.; Hicks, K. B.; Powell, M. J. Modulation of lipoxygenase activity by bacterial hopanoids. *J. Nat. Prod.* **1997**, *60*, 397–398.

[xix] Kenyon, V.; Chorny, I.; Carvajal, W. J.; Holman, T. R.; Jacobson, M. P. Novel human lipoxygenase inhibitors discovered using virtual screening with homology models. *J. Med. Chem.* **2006**, *49*, 1356–1363.

[xx] Deschamps, J. D.; Gautschi, J. T.; Whitman, S.; Johnson, T. A.; Gassner, N. C.; Crews, P.; Holman, T. R. Discovery of platelet-type 12-human lipoxygenase selective inhibitors by high-throughput screening of structurally diverse libraries, *Bioorg. Med. Chem.* **2007**, *15*, 6900-6908.

[xxi] Kenyon, V.; Rai, G.; Jadhav, A.; Schultz, L.; Armstrong, M.; Jameson, J. B.; Perry, S.; Joshi, N.; Bougie, J. M.; Leister, W.; Taylor-Fishwick D. A.; Nadler, J. L.; Holinstat, M.; Simeonov, A.; Maloney, D. J.; Holman, T. R. Discovery of Potent and Selective Inhibitors of Human Platelet-Type 12-Lipoxygenase. *J. Med. Chem.* **2011**, *54*, 5485-5497.

[xxii] (a) Fulp, A. B.; Johnson, M. S.; Markworth, J.; Marron, B. E.; Seconi, D. C.; West, C. W.; Wang, X.; Zhou, S. Sodium Channel Blockers. US Patent WO/2009/012242, Jul. 14, 2008. (b) Lee, Y. K.; Parks, D. J.; Lu, T.; Thieu, T. V.; Markotan, T.; Pan, W.; McComsey, D. F.; Milkiewicz, K. L.; Crysler, C. S.; Ninan, N.; Abad, M. C.; Giardino, E. C.; Maryanoff, B. E.; Damiano, B. P.; Player, M. R. *J. Med. Chem.* **2008**, *51*, 282-297.

[xxiii] Wang, X.; Guram, A.; Ronk, M.; Milne, J. E.; Tedrow, J. S.; Faul, M. M. Copper-catalyzed N-arylation of sulfonamides with aryl bromides. *Tetrahedron Lett.* **2012**, *53*, 7-10.

[xxiv] Gan, Q.-F.; Browner, M. F.; Sloane, D. L.; Sigal, E. Defining the arachidonic acid binding site of human 15-lipoxygenase. *J. Biol. Chem.* **1996**, *271*, 25412-25418

[xxv] Hoobler, E. K.; Holz, C.; Holman, T. R. Pseudoperoxidase investigations of hydroperoxides and inhibitors with human lipoxygenases. *Bioorg. Med. Chem.* **2013**, *21*, 3894-3899.

xxvi Rai, G.; Kenyon, V.; Jadhav, A.; Schultz, L.; Armstrong, M.; Jameson, J. B. III.; Hoobler, E.; Leister, W.; Simeonov, A.; Holman, T. R.; Maloney, D. J. *J. Med. Chem.* **2010**, *53*, 7392-7404.

xxvii Ikei, K. N.; Yeung, J.; Apopa, P. L.; Ceja, J.; Vesci, J.; Holman, T. R., Holinstat, M. Investigations of human platelet-type 12-Lipoxygenase:role of lipoxygenase products in platelet activation. *J. Lipid Res.* **2012**, *53*, 2546-2559.

xxviii (a) Thomas, C. P.; Morgan, L. T.; Maskrey, B. H.; Murphy, R. C; Kuhn, H.; Hazen, S. L.; Goodall, A. H.; Hamali, H. A.; Collins, P. W.; O'Donnell, V. D. Phospholipid-esterified eicosanoids are generated in agonist-activated human platelets and enhance tissue factor-dependant thrombin generation. *J. Biol. Chem.* **2010**, 285, 6891-6903. (b) Yeung, J.; Apopa, P. L.; Vesci, J.; Stolla, M.; Rai, G.; Simeonov, A.; Jadhav, A.; Fernandez-Perez, P.; Maloney, D. J.; Boutaud, O.; Holman, T. R.; Holinstat, M. 12-Lipoxygenase activity plays an important role in PAR4 and GPVI-mediated platelet reactivity. *Thromb. Haemost.* **2013**, *110*, 561-581.

xxix Yeung, J.; Apopa, P. L.; Vesci, J.; Kenyon, V.; Rai, G.; Jadhav, A.; Simeonov, A.; Holman, T R.; Maloney, D. J.; Boutaud O, Holinstat M Protein kinase C regulation of 12-lipoxygenase-mediated human platelet activation. *Mol Pharm* **2012**, *81*, 420-430.

xxx Ma, K.; Nunemaker, C. S.; Wu, R.; Chakrabarti, S. K.; Taylor-Fishwick, D. A.; Nadler, J. L. 12-Lipoxygenase Products Reduce Insulin Secretion and β-cell Viability in Human Islets. *J. Clin. Endocrinol. Metab.* **2010**, *95*, 887-893.

xxxi Madsen, P.; Ling, A.; Plewe, M.; Sams, C. K.; Knudsen, L. B.; Sidelmann, U. G.; Ynddal, L.; Brand, C. L.; Andersen, B.; Murphy, D.; Teng, M.; Truesdale, L.; Kiel, D.; May, J.; Kuki, A.; Shi, S.; Johnson, M. D.; Teston, K. A.; Feng, J.; Lakis, J.; Anderes, K.; Gregor, V.; Lau, J. Optimization of Alkylidene Hydrazide Based Humna Glucagon Receptor Antagonists. Discovery of the Highly Potent and Orally Available 3-Cyano-4-hydroxybenzoic Acid [1-(2,3,5,6-Tetramethylbenzyl)-1*H*-indol-4-ylmethylene]hydrazide. *J. Med. Chem.* **2002**, *45*, 5755-5775.

xxxii Ettmayer, P.; Amidon, G. L.; Clement B.; Testa, B. Lessons learned from marketed and investigational prodrugs. *J. Med. Chem.* **2004**, *47*, 2393-2404.

xxxiii (a) Amagata, T.; Whitman, S.; Johnson, T. A.; Stessman, C. C.; Loo, C. P.; Lobkovsky, E.; Clardy, J.; Crews, P.; and Holman, T. R. Exploring sponge-derived terpenoids for their potency and selectivity against 12-human, 15-human, and 15-soybean lipoxygenases, *J. Nat. Prod.* **2003**, *66*, 230-235. (b) Ohri, R. V.; Radosevich, A. T.; Hrovat, K. J.; Musich, C.; Huang, D.; Holman, T. R.; Toste, F. D. A Re(V)-catalyzed C-N bond-forming route to human lipoxygenase inhibitors, *Org. lett.* **2005**, *7*, 2501-2504. (c) Chen, X.-S.; Brash, A.; and Funk, C. Purification and characterization of recombinant histidine-tagged human platelet 12-lipoxygenase expressed in a baculovirus/insect cell system. *Eur. J. Biochem.* **1993**, *214*, 845-852.

xxxiv Robinson, S. J.; Hoobler, E. K.; Riener, M.; Loveridge, S. T.; Tenney, K.; Valeriote, F. A.; Holman, T. R.; Crews, P. Using enzyme assays to evaluate the

structure and bioactivity of sponge-derived meroterpenes. *J. Nat. Prod.* **2009**, *72*, 1857-1863.

[xxxv] Inglese, J.; Auld, D. S.; Jadhav, A.; Johnson, R. L.; Simeonov, A.; Yasgar, A.; Zheng, W.; Austin, C. P. Quantitative High-Throughput Screening: A Titration-Based Approach That Efficiently Identifies Biological Activities in Large Chemical Libraries. *Proc. Natl. Acad. Sci. U.S.A.* **2006**, *103*, 11473–11478.